Engineering swollen cubosomes using cholesterol and anionic lipids.

Hanna M.G. Barriga†, Oscar Ces, Robert V. Law, John M. Seddon and Nicholas J. Brooks*.*

Department of Chemistry, Imperial College London, Molecular Sciences Research Hub, White City Campus, Wood Lane, W12 0BZ, UK.

ABSTRACT: Dispersions of non-lamellar lipid membrane assemblies are gaining increasing interest for drug delivery and protein therapeutic application. A key bottleneck has been the lack of rational design rules for these systems linking different lipid species and conditions to defined lattice parameters and structures. We have developed robust methods to form cubosomes (nanoparticles with a porous internal structure) with water channel diameters of up to 171 Å which are over 4 times larger than archetypal cubosome structures. The water channel diameter can be tuned via the incorporation of cholesterol and the charged lipids DOPA, DOPG or DOPS. We have found that large molecules can be incorporated into the porous cubosome structure and these molecules can interact with the internal cubosome membrane. This offers huge potential for accessible encapsulation and protection of biomolecules, and development of confined interfacial reaction environments.

INTRODUCTION: Cells are complex assemblies of lipids, proteins and a wide range of other molecules, which govern compartmentalization, regulation of cellular content and signaling

pathways.[1] It can be difficult to engineer therapeutic agents that interact with cellular systems specifically and efficiently; however, model membrane based carriers can significantly enhance drug efficacy due to their biocompatible lipid composition which can lead to increased uptake and lower toxicity. Model membranes also offer opportunities for targeting via incorporation of bioactive lipids and antibody labelling to increase specificity.[2] To date the majority of lipid based therapeutic agents are vesicular.[3,4,5] Vesicular systems are based on mixtures of lipids which form a single bilayer envelope surrounding an aqueous internal volume. Increasingly, lipid nanoparticles with non-lamellar internal membrane structures are gaining significant attention.[6,7] A key advantage of these systems in comparison to vesicles, is their much higher membrane surface area to volume ratio; this is extremely important in increasing loading, containment and protection of interfacial active cargo.

The majority of examples of non-lamellar dispersions are cubosomes, which are particles of a few hundred nm in size formed from dispersions of lipid bicontinuous cubic phases in the presence of a stabilizing polymer. There are three different lipid bicontinuous cubic phases with Ia3d, Im3m and Pn3m symmetry ($Q_{II}G$, $Q_{II}P$ and $Q_{II}D$ respectively),[8–11] and they are all formed by a single lipid bilayer draped over an infinite periodic minimal surface which separates two independent but intertwined water channel networks. They are formed via self-assembly and their properties are tunable via compositional, pressure and temperature variation.[12,13] There is already significant research into different stabilizers, and their effects on toxicity, uptake and cubosome structure.[14–17] These stabilizers provide a library of compounds for targeting cubosomes through biofunctionalisation and antibody targeting.[18,19]

Demurtas et al. have directly visualized cubosome dispersions formed from monoolein and a polyglycerol ester using cryo electron tomography. This work suggests that the internal cubic

structure is effectively defect free and that at least one channel network is isolated from the surrounding aqueous environment.[20]

Whilst many examples of cubosomes exist in the literature, the majority of these are formed from single or binary lipid mixtures.[21,22] They have been used in applications including loading of small drug molecules for cancer therapy, drug delivery via lipase digestion, testing lipolytic enzyme activity and acting as potentiators for the delivery of immunostimulants.[23–29] However, there are very few examples of cubosomes with larger molecule and protein cargo due to severe limitations in currently attainable pore sizes.[30] Conn et al. have demonstrated loading of the dopamine D2L receptor into monoolein and phytantriol cubosomes doped with Ni(II) chelated EDTA amphiphiles,[31] Zabara et al. have demonstrated pH responsive cubosomes with Outer Membrane Protein F (OmpF) reconstituted into the bilayer[32] and Rodrigues et al. have loaded phytantriol hexasomes with lysozyme and ovalbumin.[33] Cubosomes have been loaded with beta casein[34] for release of nerve growth factor in PC12 cells[35] and more recently intravenously injected dye loaded cubosomes have been used for in-vivo lifetime imaging in mice.[36] These are highly encouraging developments but there remains a significant bottleneck in the wider application of cubosomes due to the lack of methods to produce them with large, well defined water channel diameters. High throughput production techniques have also been lacking although recent progress demonstrating progress towards on-chip formulations for cubosomes and lipid nanoparticles with further expand their application.[37,38]

Problems controlling bulk cubic phases for crystallization of membrane proteins[39,40] have now been overcome and highly swollen bulk bicontinuous cubic phases with lattice parameters of up to 480 Å and water channel diameters of almost 250 Å have been reported in mixtures of monoolein, cholesterol and anionic lipid.[12,13] This was achieved by addition of cholesterol, which

stiffens the bilayer and reduces thermal fluctuations, and charged lipids to electrostatically swell the structure. Leung et al. have also shown that ternary mixtures of monoolein, DOTAP and DOPE-PEG (95:4:1 MO:DOTAP/DOPE-PEG) can form highly swollen primitive cubic phases with lattice parameters of up to 484 Å.[41] These engineering principles have been used to design swollen lipid cubic phases for the crystallization of the Gloeobacter violaceus ligand-gated ion channel (GLIC) which contains large extracellular domains which was impossible in non-swollen cubic phases.[42]

There is evidence that cubosomes formed from lipid mixtures that include a charged component can exhibit increased water channel sizes. Two of the largest reported examples have used cationic lipids and include Angelova et al. who incorporated 15 mol% of DOMA and 3 mol% of DOPE.PEG2000 into monoolein cubosomes resulting in mixed Pn3m-Im3m phase coexistences with lattice parameters of 283 and 349 Å, respectively[43] and Leal et al. who incorporated 15 mol% DOTAP resulting in a lattice parameter of over 200 Å at 60 wt% water.[44] Leal et al. also demonstrated cubosome loading with siRNA for gene silencing and that the geometry of the these nanoparticles can enhance delivery in comparison to liposome systems.[44,45] However, all of the work to date offers very limited targeting of the cubosome structure. Here we report a library of highly swollen cubosome dispersions formed from ternary mixtures including monoolein (MO), cholesterol (CHOL) and an anionic lipid component: 1,2-dioleoyl-sn-glycero-3-phospho-L-serine (sodium salt) (DOPS), 1,2-dioleoyl-sn-glycero-3-phospho-(1'-rac-glycerol) (sodium salt) (DOPG) or 1,2-dioleoyl-sn-glycero-3-phosphate (sodium salt) (DOPA) and stabilized with F-127.

These dispersions have lattice parameters of up to 339 Å and pore sizes of up to 171 Å. By changing the lipid type and percentage of anionic lipid incorporated, the lattice parameter and

pore sizes can be precisely controlled. The cubosome assemblies have been characterized by small angle X-ray diffraction (SAXS) and cryo transmission electron microscopy (Cryo TEM) providing a detailed understanding of both their internal structure and particle morphology. We further show via a fluorescence based assay that Lectin PHA-L, a tetrameric protein of 120 kDa, can be encapsulated into the cubosomes' membrane bound water channels based on the channel pore size. This work vastly expands the structural parameter space that we can access in cubosome systems and offers potential for large protein therapeutic encapsulation and delivery.

EXPERIMENTAL:

Materials

1,2-dioleoyl-sn-glycero-3-phospho-L-serine (sodium salt) (DOPS), 1,2-dioleoyl-sn-glycero-3-phospho-(1'-rac-glycerol) (sodium salt) (DOPG), 1,2-dioleoyl-sn-glycero-3-phosphate (sodium salt) (DOPA), 1,2-dioleoyl-sn-glycero-3-phosphocholine (DOPC), 1,2-dioleoyl-sn-glycero-3-phosphoethanolamine-N-(lissamine rhodamine B sulfonyl) (ammonium salt) (Liss Rhod PE) and cholesterol (ovine, wool) (CHOL) were purchased from Avanti Polar Lipids (AL, USA) as lyophilised powders. 1-Oleoyl-rac-glycerol (monoolein, MO) and potassium chloride, (KCl) and chloroform were purchased from Sigma Aldrich (Gillingham, UK). DOPS, DOPG, DOPA, CHOL and MO lipids had a purity of >98% and were used without further purification, but were lyophilised for 12 hours before use to ensure they were fully dry. Lectin PHA-L From Phaseolus vulgaris (red kidney bean) (Lectin PHA-L), Alexa Fluor 488 Conjugate was purchased from Thermo Fisher Scientific as a lyophilized powder and hydrated to 1 mg/ml in 100mM KCl, aliquoted and stored at -20°C.

Cubosome preparation

Lipid mixtures were formed by co-dissolving the lipids at the relevant mol% ratios in chloroform followed by solvent removal under a stream of nitrogen gas to form a lipid film and a minimum of 4 hours on the lyophiliser to remove residual chloroform. Lipid films were hydrated in 100mM KCl, pH 7.4 (sterile filtered) to 50mM and homogenised via a minimum of 15 freeze thaw cycles between approximately -196°C and 60°C. Samples were subsequently heated to 25°C and 1ml of 2mg/ml F-127 solution in 100mM KCl was added prior to sonication using a VibraCell VCX 750 with a tapered microtip using pulse mode (1s on, 1s off), amplitude 30%, for a maximum of 5 minutes. Residual titanium from the sonication tip was removed via centrifugation 4000 rpm for 10 minutes in an Eppendorf benchtop centrifuge. Dynamic light scattering of the cubosome samples composed of MO, MO:CHOL:DOPS 60:30:5 mol% and MO:CHOL:DOPS 60:30:10 mol% showed a single peak with a PDI below 0.2 as shown in Supporting Information Figure S1. All cubosome samples were used within 1 day of formation.

SAXS preparation

Cubosomes were loaded into glass capillaries which were sealed with silicon sealant and imaged in a temperature controlled capillary holder. Where necessary cubosome samples were concentrated using Amicon centrifugal concentrators with a 100K MWCO. Data was collected at the European Synchrotron Radiation Facility (ESRF) using beamline ID02. Diffraction patterns were collected using an X-ray wavelength of 0.73 Å and at a camera lengths of 1m or 6m. Images were analysed using the in-house developed software package AXcess.[46] Briefly, the two dimensional SAXS patterns were radially integrated to give one dimensional diffraction patterns. The Bragg peaks were then fitted using Gaussian functions and indexed by comparison to characteristic diffraction patterns from known lipid structures. These fits were used to calculate the lattice parameters.

Cryo-TEM

Cubosomes were formed as previously described with a composition of MO:CHOL:DOPS 60:30:10 mol%, diluted 1:10 in 100mM KCl and 2µl pipetted immediately onto glow discharged holey carbon grids (Quantifoil R 2/2). Grids were vitrified in liquid ethane with an FEI Vitribot with an offset of -4 and a wait and blot time of 5s. Grids were stored in liquid nitrogen prior to Cryo TEM image acquisition on a 120kV FEI Tecnai 12 with an F216 TVIPS CCD camera. Images were recorded with a magnification of 30,000x, a defocus of -1.6µm and an electron dose of 1845 e^-/nm^2. Raw images were imported into ImageJ for processing. FFT analysis was performed in ImageJ by selecting regions of interest and using the FFT function. Brightness and contrast was enhanced in some images for the purposes of clearer viewing. Scale bars have been added to the images using ImageJ.

Fluorescence FRET Assay

Cubosomes were prepared as described previously with 0.1 mol% Liss Rhod PE co-lyophilised with the lipid mixture prior to solvent removal. Suitable concentrations of cubosomes and Lectin PHA-L were optimised via dilution in 100mM KCl in a Varian Cary Eclipse fluorimeter to give a final lipid:protein ratio of 1000:1. The sample was excited at 495nm and the FRET was calculated by taking the fluorescence at 590 nm, which corresponds to the lipid fluorescence and dividing by the sum of the fluorescence at 520nm and 590nm which correspond to the lectin PHA-L and lipid respectively.

$$FRET = \frac{lipid\ fluorescence_{590nm}}{lipid\ fluorescence_{590nm} + lectin\ PHAL\ fluorescence_{520nm}}$$

Samples were subsequently diluted 1:1 in 100mM KCl three times and the FRET measured at each point to ascertain if trapping of the protein had occurred. Data shown is the mean and standard error of three measurements. As a control, vesicles were formed with an identical lipid and Rhod PE concentration to the cubosome mixture by preparing the films as described previously, freeze-thawing followed by extrusion through a 100nm polycarbonate filter using an Avanti Mini Extruder. Vesicle FRET experiments were repeated in an identical manner to the cubosome experiments.

RESULTS: Previous work on bulk monoolein based bicontinuous cubic phases in water showed electrostatic swelling of the cubic phase above the limits previously predicted by Bruinsma et al.[47] The extremely high water channel diameter porous cubosome nanoparticles developed here follow very similar design rules to their bulk structure counterparts (electrostatic swelling achieved by incorporation of charged lipids coupled to membrane stiffening by cholesterol). Figure 1 a-d shows the lattice parameters of cubosomes formed with different lipid compositions and representative small angle diffraction patterns from the cubosome dispersions are shown in Supporting Information Figure S2.

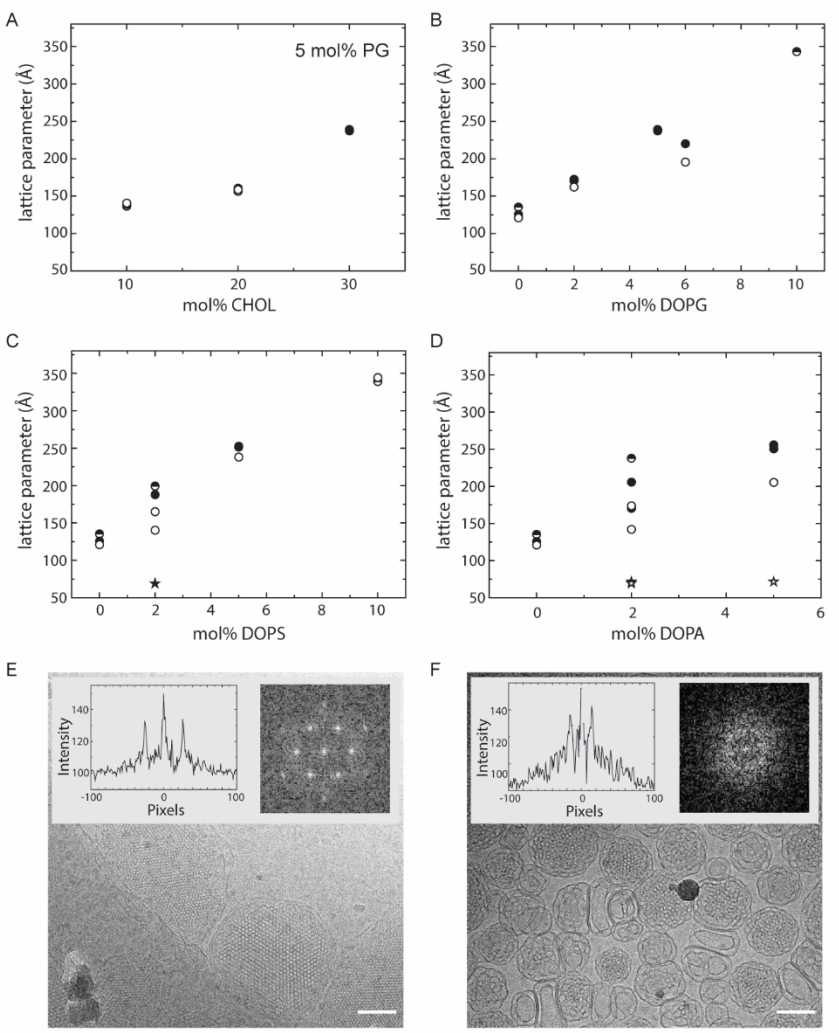

Figure 1. Im3m bicontinuous cubic phase (except ★ H_{II} 37°C, ☆ H_{II} 45°C) SAXS lattice parameters of cubosomes formed in 100mM KCl showing the effects of temperature (◓ 25°C, ● 37°C, ○ 45°C) and composition of (a) CHOL in cubosomes containing 5 mol% DOPG, (b) DOPG in cubosomes containing 30 mol% CHOL, (c) DOPS in cubosomes containing 30 mol% CHOL (d) DOPA in cubosomes containing 30 mol% CHOL. Each data point corresponds to an individual sample and the estimated error is smaller than the data points. The 0 mol% anionic lipid points have been included for comparison and correspond to pure monoolein. Cryo TEM

images of cubosomes formed from (e) 100% MO (f) MO:CHOL:DOPS 55:30:10 mol% in 100mM KCl, with power spectra and radial integrations shown inset. Scale bars are 100 nm.

The effect of cholesterol on the lattice parameter of MO:CHOL:DOPG cubosomes in 100mM KCl with 5 mol% DOPG can be seen in Figure 1a. The cubosomes have an internal Im3m structure and increasing the cholesterol from 10 to 30 mol% causes the lattice parameter to increase from 137 Å to 239 Å at 25 °C. Increasing the temperature to 37 °C and subsequently 45 °C led to comparatively small lattice parameter changes (< 5 Å). Bulk mixtures containing 5 mol% DOPG and 70 wt% water at 35°C exhibit a lattice parameter of 361 Å at 0 mol% cholesterol, which increased to a maximum of 415 Å at 15 mol% cholesterol. At 45 °C, the lattice parameter of the bulk Im3m phase swells from 364 Å at 0 mol% cholesterol to 423 Å at 30 mol% cholesterol.[12] The lattice parameter trend of the bulk mixtures corresponds well to the cubosome behavior we report, however, in cubosomes containing 5 mol% DOPG we do not observe the coexisting hexagonal (H_{II}) phase at 45 °C seen in the bulk mixtures. It is likely that the F-127 shifts the phase boundaries. Cubosomes in water with increasing mol% of cholesterol in the absence of charged lipid also exhibited Im3m phase morphology (Supporting Information Figure S3). The lattice parameter we report in the cubosome system at 30 mol% cholesterol and 5 mol% DOPG in 100mM KCl is approximately 100 Å smaller than that reported in the bulk system in water.[12] We attribute this to the presence of buffer leading to some electrostatic screening of the headgroup charges and reducing the long range electrostatic swelling of the cubic phase. As the incorporation of cholesterol increased the lattice parameter of ternary lipid cubosomes without disrupting the structure, all further cubosomes were formed with 30 mol% cholesterol. This concentration was set just above the 28 mol% solubility limit of cholesterol in pure monoolein.[48]

The effects of adding the anionic lipids DOPG, DOPS, and DOPA to cubosomes can be seen in Figure 1b-d. In all cases increasing the mol% of charged lipid increased the lattice parameter. For DOPG and DOPS at 25°C, increasing the anionic lipid from 2 to 10 mol% increased the lattice parameter by 172 and 140 Å, respectively. DOPA was only measured up to 5 mol%, which exhibited a cubic lattice parameter of 256 Å and at higher temperatures, coexistence of an H_{II} phase. These trends correspond well to the electrostatic swelling of lattice parameters in bulk ternary mixtures and demonstrate that cubosomes can also be engineered for pore size and composition. We did not observe the lamellar phase transitions observed in the bulk mixture at 10 mol%, potentially due to the buffer and stabilizer shifting the phase boundaries. Some lattice parameter changes were seen as the temperature was increased to 37°C and 45°C, although these were small in comparison to the differences seen with anionic lipid. Samples containing DOPS and DOPA showed an H_{II}-Im3m phase coexistence at 45°C resulting in a shrinking of the Im3m cubic phase. This was also visible in the DOPA sample from 37°C. The occurrence of the H_{II} phase was reversible upon cooling.

Table 1. Estimated channel widths for the Im3m phase of the most swollen cubosome structures at 25°C. Where a is the Im3m lattice parameter, R_W is the water channel radius.

Sample (mol%)	**a (Å)**	**R_w (Å)**
MO	135	23
MO:CHOL:PA 65:30:5	256	60
MO:CHOL:PG 60:30:10	343	87
MO:CHOL:PS 60:30:10	339	85

Table 1 shows estimated water channel diameters for the cubosomes with the largest observed lattice parameters. These have been calculated using equation 1 derived by Briggs et al.[49,50]

$$R_W = 0.305a - L \qquad \text{(equation 1)}$$

Where R_W is the water channel radius, a is the lattice parameter and L is the monolayer thickness of MO in the Pn3m phase which was taken to be 18 Å.[51] It should be noted that these are estimates as the samples also contain F-127 and in most cases cholesterol and charged lipids for which monolayer thicknesses are not available. By electrostatically swelling the cubosomes' internal structure we can achieve water channel diameters exceeding 170 Å and achieve rational design of cubosome systems with defined pore sizes in buffer making them compatible with a wide range of protein and other biomolecular encapsulation applications.

Representative Cryo-TEM images of MO:CHOL:DOPS 60:30:10 mol% cubosomes in 100mM KCl are shown in Figure 1e-f with fast Fourier transforms (FFT) (inset) highlighting the cubosome's internal structure. Radial integrations of the power spectra are also shown and demonstrate the shift in peak position corresponding to the larger pore sizes. The Cryo-TEM images show some pore size distribution in the DOPS cubosomes which was not observed in the SAXS data. The Cryo TEM data represents individual cubosomes within the sample and the grid preparation can favor larger, denser particles due to the wait time prior to blotting in which the particles settle. This process is likely to accentuate the observed pore size distribution and the absence of significant polydispersity in the SAXS data (which samples a large cross section of the sample) indicates that bulk of the cubosomes adopt a well defined pore size.

One of the most important potential application of cubosomes is for the encapsulation of proteins. To demonstrate this in swollen pore size systems, a FRET assay was developed to test protein incorporation into cubosomes formed from pure MO and MO:CHOL:DOPS 60:30:10 mol%. Rhodamine B labelled lipid (Rh-DHPE) was incorporated into the membrane and Alexa 488 labelled lectin PHA-L was added externally. A schematic of this assay can be seen in Figure

2a-c. The FRET, defined in the experimental section, was 0.23 +/- 0.01 in MO cubosomes in comparison to the swollen cubosomes containing 30 mol% CHOL and 10 mol% DOPS which showed a FRET value of 0.32 +/- 0.01. Upon 1:1 dilution of the samples with buffer, the FRET signal decreased in both cases. The larger FRET value measured for the MO:CHOL:DOPS cubosomes in comparison to the MO cubosomes is indicative of a greater access to the internal membrane due to an increase in channel size. Assuming that the protein membrane interaction is similar in both cases, the FRET signal will be proportional to the number of PHA-L proteins able to interact with the lipid membrane. In this case, the 40% increase in the FRET signal when the channel diameter increases from 46 Å in the MO system to 171 Å in the MO:CHOL:DOPS system implies approximately a 40% increase in the protein accessible membrane area. Decreasing FRET upon dilution is attributed to reduced surface association and indicates the lectin-PHA-L is not trapped within the larger pores. The hydrodynamic radius of Lectin-PHAL is approximately 42 Å.[52] The diameter of the water channels in MO cubosomes is estimated to be 46 Å (Table 1). Therefore it is conceivable that the lectin PHA-L has some limited access to the water channels and therefore cubic membrane in the MO only case as well as the MO:CHOL:DOPS cubosome which explains the non-zero FRET. However, as the hydrodynamic radius of lectin-PHA-L and the MO channel diameter are almost identical, proteins loaded close to the particle surface are likely to block access via the water channel network to the particle core. When the water channels swell with the addition of DOPS, the channels are 3.7 times larger and therefore free diffusion of protein within the water channel network would still be possible even if loading occurs close to the particle surface leading to increased protein loading and an increase in the measured FRET signal.

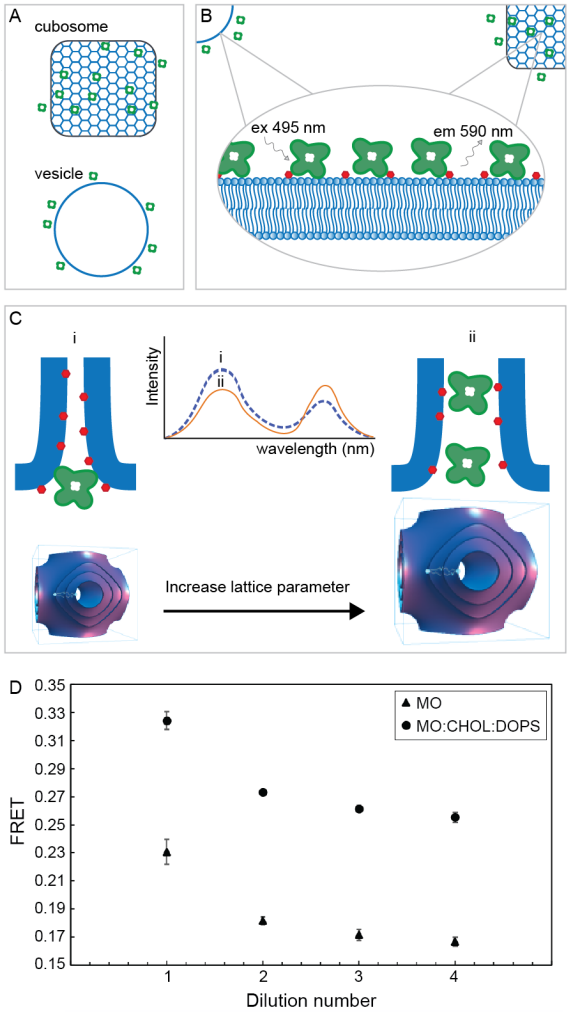

Figure 2. FRET assay for Lectin PHA-L (Alexa 488) interacting with Rh-DHPE in the lipid membrane. Schematics shown demonstrate a) association of lectin PHA-L with vesicle and cubosome membranes b) FRET in a vesicle and cubosome c) how FRET is affected by a swelling of the water channel size d) FRET assay results comparing MO (▲) and MO:CHOL:DOPS (●) cubosome FRET in charged and neutral systems.

To compare FRET in the cubosomes with a system where the lectin PHA-L has access to a known membrane surface area, FRET experiments for vesicles with identical lipid and Rh-DHPE concentrations for DOPC:CHOL 70:30 mol% and DOPC:CHOL:DOPS 60:30:10 mol%

were performed. Results are shown in Supporting Information Figure S4. FRET values obtained were very similar to those obtained for the MO:CHOL:DOPS cubosomes. In a vesicle, the lectin PHA-L has access to approximately 50% of the lipid molecules, those on the vesicle outer surface. This implies that in the MO:CHOL:DOPS system, the lectin PHA-L must have access to a similar proportion of lipid molecules. This is only possible if the protein can access the internal cubosome membrane as the total number of lipid molecules in the two experiments are identical. Previous studies have indicated that at least one of the channel networks in cubosome systems is open.[20] Interestingly the similarity in FRET values obtained between the vesicle and cubosome systems may support the hypothesis that for large molecules one channel network is open and the other closed i.e. that in both the vesicle and the MO:CHOL:DOPS systems only 50% of the lipid molecules (one leaflet) is accessible. Assuming an excess of protein, if both channels were open the protein would be able to access all lipid molecules in the cubosomes and the corresponding FRET signal would be approximately double that observed for the vesicle sample. Establishing these engineering rules will enable us to tailor water channel size to the desired cargo to maximize loading efficiency i.e. to have the smallest water channel size feasible to maximize membrane surface area. It is possible that a similar FRET assay could be used to quantify loading of proteins, however this is outside the scope of this study.

CONCLUSIONS: In conclusion we show that cubosomes with defined channel sizes can be engineered using monoolein, cholesterol and up to 10 mol% anionic lipid. Cholesterol swells the membrane with further addition of charged lipids leading to an electrostatic swelling of the bilayer. This data is in good agreement with previous investigations into swelling bicontinuous cubic phases in bulk and shows that cubosomes can be systematically designed and engineered using lipid compositions and channel sizes tailored to specific applications. Furthermore, our

FRET data shows that a relatively large protein can access the cubosome internal membrane to a significantly greater extent in swollen cubosomes than those with smaller pore sizes. Swollen cubosomes offer a versatile platform for protein encapsulation and an exciting alternative to vesicular delivery systems with significantly higher membrane area, and potential for dynamic control of the cubosome pore size, accessibility and release characteristics. This unlocks the possibility of using cubosomes for a variety of applications including enzymatic reactions, protein trapping and protein therapeutics.

ASSOCIATED CONTENT

Supporting Information.

The Supporting Information includes: DLS data, example SAXS patterns, SAXS data on cholesterol incorporation into cubosomes and additional FRET data. The following files are available free of charge. (Barriga Langmuir SI.pdf)

AUTHOR INFORMATION

Corresponding Author

* email: hanna.barriga@ki.se or n.brooks@imperial.ac.uk

Present Addresses

† Current address: Department of Medical Biochemistry and Biophysics, Karolinska Institutet, SE 171 77 Stockholm, Sweden.

Author Contributions

The manuscript was written through contributions of all authors. All authors have given approval to the final version of the manuscript.

Notes

The authors declare no competing financial interests.

ACKNOWLEDGMENT

We acknowledge the ESRF (beamline ID2, SC-4081) and Diamond Light Source (beamline I22, SM14217) for the award of synchrotron beamtime and would like to thank Dr Johannes Moeller (ESRF) and Dr Olga Shebanova (Diamond) for their support and assistance in using the beamlines. This work was supported by EPSRC Programme Grant EP/J017566/1.

ABBREVIATIONS

MO, monoolein; CHOL, cholesterol; DOPS, 1,2-dioleoyl-sn-glycero-3-phospho-L-serine (sodium salt); DOPG, 1,2-dioleoyl-sn-glycero-3-phospho-(1'-rac-glycerol) (sodium salt); DOPA, 1,2-dioleoyl-sn-glycero-3-phosphate (sodium salt); DOPC, 1,2-dioleoyl-sn-glycero-3-phosphocholine; SAXS, small angle X-ray diffraction; Cryo TEM, cryo transmission electron microscopy; FFT, fast Fourier transforms; FRET, Förster resonance energy transfer

REFERENCES

(1) van Meer, G.; Voelker, D. R.; Feigenson, G. W. Membrane Lipids: Where They Are and How They Behave. *Nat. Rev. Mol. Cell Biol.* **2008**, *9* (2), 112–124. https://doi.org/10.1038/nrm2330.

(2) Puri, A.; Loomis, K.; Smith, B.; Lee, J.; Yavlovich, A.; Heldman, E.; Blumenthal, R. Lipid Based Nanoparticles as Pharmaceutical Drug Carriers. *Crit. Rev. Ther. Drug Carrier Syst.* **2009**, *26* (6), 523–580.

(3) Fassas, A.; Anagnostopoulos, A. The Use of Liposomal Daunorubicin (DaunoXome) in

Acute Myeloid Leukemia. *Leuk. Lymphoma* **2005**, *46* (6), 795–802.

(4) Boulikas, T. Clinical Overview on Lipoplatin. a Successful Liposomal Formulation of Cisplatin. *Expert Opin. Investig. Drugs* **2009**, *18* (8), 1197–1218.

(5) Meyerhoff, A. US Food and Drug Administration Approval of AmBisome (Lipo-Somal Amphotericin B) for Treatment of Visceral Leishmaniasis. *Clin. Infect. Dis.* **1999**, *28* (1), 42–48.

(6) Karami, Z.; Hamidi, M. Cubosomes: Remarkable Drug Delivery Potential. *Drug Discov. Today* **2016**, *21* (5), 789–801.

(7) Azmi, I.; Moghimi, S.; Yaghmur, A. Cubosomes and Hexasomes as Versatile Platforms for Drug Delivery. *Ther. Deliv.* **2015**, *6* (12), 1347–1364.

(8) Seddon, J. M. Structure of the Inverted Hexagonal (HII) Phase, and Non-Lamellar Phase Transitions of Lipids. *Biochim. Biophys. Acta* **1990**, *1031* (1), 1–69.

(9) Kim, H.; Song, Z.; Leal, C. Super-Swelled Lyotropic Single Crystals. *Proc. Natl. Acad. Sci. U. S. A.* **2017**, *114* (41), 10834–10839. https://doi.org/10.1073/pnas.1710774114.

(10) Conn, C. E.; Drummond, C. J. Nanostructured Bicontinuous Cubic Lipid Self-Assembly Materials as Matrices for Protein Encapsulation. *Soft Matter* **2013**, *9* (13), 3449. https://doi.org/10.1039/c3sm27743g.

(11) Tan, A.; Hong, L.; Du, J. D.; Boyd, B. J. Self-Assembled Nanostructured Lipid Systems: Is There a Link between Structure and Cytotoxicity? *Adv. Sci.* **2019**, *6* (3), 1801223. https://doi.org/10.1002/advs.201801223.

(12) Tyler, A. I. I.; Barriga, H. M. G.; Parsons, E. S.; McCarthy, N. L. C.; Ces, O.; Law, R. V.; Seddon, J. M.; Brooks, N. J. Electrostatic Swelling of Bicontinuous Cubic Lipid Phases. *Soft Matter* **2015**, *11*, 3279–3286.

(13) Barriga, H. M. G.; Tyler, A. I. I.; McCarthy, N. L. C.; Parsons, E. S.; Ces, O.; Law, R. V.; Seddon, J. M.; Brooks, N. J. Temperature and Pressure Tuneable Swollen Bicontinuous Cubic Phases Approaching Nature's Length Scales. *Soft Matter* **2015**, *11*, 600–607.

(14) Chong, J. Y. T.; Mulet, X.; Postma, A.; Keddie, D. J.; Waddington, L. J.; Boyd, B. J.; Drummond, C. Novel RAFT Amphiphilic Brush Copolymer Steric Stabilisers for Cubosomes: Poly(Octadecyl Acrylate)- Block-Poly(Polyethylene Glycol Methyl Ether Acrylate). *Soft Matter* **2014**, *10*, 6666–6676.

(15) Chong, J. Y. T.; Mulet, X.; Waddington, L. J.; Boyd, B. J.; Drummond, C. Steric Stabilisation of Self-Assembled Cubic Lyotropic Liquid Crystalline Nanoparticles: High Throughput Evaluation of Triblock Polyethylene Oxide-Polypropylene Oxide-Polyethylene Oxide Copolymers. *Soft Matter* **2011**, *7* (4768–4777).

(16) Chong, J. Y. T.; Mulet, X.; Waddington, L. J.; Boyd, B. J.; Drummond, C. High-Throughput Discovery of Novel Steric Stabilizers for Cubic Lyotropic Liquid Crystal Nanoparticle Dispersions. *Langmuir* **2012**, *28* (9223–9232).

(17) Zhai, J.; Suryadinata, R.; Luan, B.; Tran, N.; Hinton, T.; Ratcliffe, J.; Hao, X.; Drummond, C. Amphiphilic Brush Polymers Produced Using the RAFT Polymerisation Method Stabilise and Reduce the Cell Cytotoxicity of Lipid Lyotropic Liquid Crystalline Nanoparticles. *Faraday Discuss*. **2016**, *191* (545–563).

(18) Fraser, S. J.; Mulet, X.; Martin, L.; Praporski, S.; Mechler, A.; Hartley, P. G.; Polyzos, A.; Separovic, F. Surface Immobilization of Bio-Functionalized Cubosomes: Sensing of Proteins by Quartz Crystal Microbalance. *Langmuir* **2012**, *28* (1), 620–627.

(19) Zhai, J.; Scoble, J. A.; Li, N.; Lovrecz, G.; Waddington, L. J.; Tran, N.; Muir, B. W.; Coia, G.; Kirby, N.; Drummond, C.; et al. Epidermal Growth Factor Receptor-Targeted Lipid Nanoparticles Retain Self-Assembled Nanostructures and Provide High Specificity. *Nanoscale* **2015**, *7* (2905–2913).

(20) Demurtas, D.; Guichard, P.; Martiel, I.; Mezzenga, R.; Herbert, C.; Sagalowicz, L. Direct Visualization of Dispersed Lipid Bicontinuous Cubic Phases by Cryo-Electron Tomography. *Nat. Commun.* **2015**, *6*, 8915.

(21) Ghazal, A.; Gontsarik, M.; Kutter, J.; Lafleur, J. P.; Labrador, A.; Mortensen, K.; Yaghmur, A. Direct Monitoring of Calcium-Triggered Phase Transitions in Cubosomes Using SAXS Combined with Microfluidics. *J. Appl. Crystallogr.* **2016**, *49* (2005–2014).

(22) Kulkarni, C. V; Yaghmur, A.; Steinhart, M.; Kriechbaum, M.; Rappolt, M. Effects of High Pressure on Internally Self-Assembled Lipid Nanoparticles : A Synchrotron Small-Angle X-Ray Scattering (SAXS) Study. *Langmuir* **2016**, *32* (11907–11917).

(23) Murgia, S.; Bonacchi, S.; Falchi, A. M.; Lampis, S.; Lippolis, V.; Meli, V.; Monduzzi, M.; Prodi, L.; Schmidt, J.; Talmon, Y.; et al. Drug-Loaded Fluorescent Cubosomes: Versatile Nanoparticles for Potential Theranostic Applications. *Langmuir* **2013**, *29* (22), 6673–6679. https://doi.org/10.1021/la401047a.

(24) Caltagirone, C.; Falchi, A. M.; Lampis, S.; Lippolis, V.; Meli, V.; Monduzzi, M.; Prodi,

L.; Schmidt, J.; Sgarzi, M.; Talmon, Y.; et al. Cancer-Cell-Targeted Theranostic Cubosomes. *Langmuir* **2014**, *30* (21), 6228–6236.

(25) Murgia, S.; Falchi, A. M.; Meli, V.; Schillen, K.; Lippolis, V.; Monduzzi, M.; Rosa, A.; Schmidt, J.; Talmon, Y.; Bizzarri, R.; et al. Cubosome Formulations Stabilized by a Dansyl-Conjugated Block Copolymer for Possible Nanomedicine Applications. *Colloids Surfaces B Biointerfaces* **2015**, *129* (87–94).

(26) Aleandri, S.; Bandera, D.; Mezzenga, R.; Landau, E. M. Biotinylated Cubosomes: A Versatile Tool for Active Targeting and Codelivery of Paclitaxel and a Fluorescein-Based Lipid Dye. *Langmuir* **2015**, *31* (46), 12770–12776.

(27) Wadsäter, M.; Barauskas, J.; Nylander, T.; Tiberg, F. Formation of Highly Structured Cubic Micellar Lipid Nanoparticles of Soy Phosphatidylcholine and Glycerol Dioleate and Their Degradation by Triacylglycerol Lipase. *ACS Appl. Mater. Interfaces* **2014**, *6* (10), 7063–7069.

(28) Barauskas, J.; Anderberg, H.; Svendsen, A.; Nylander, T. Thermomyces Lanuginosus Lipase-Catalyzed Hydrolysis of the Lipid Cubic Liquid Crystalline Nanoparticles. *Colloids Surfaces B Biointerfaces* **2016**, *137*, 50–59.

(29) Liu, Z.; Luo, L.; Zheng, S.; Niu, Y.; Bo, R.; Huang, Y.; Xing, J.; Li, Z.; Wang, D. Cubosome Nanoparticles Potentiate Immune Properties of Immunostimulants. *Int. J. Nanomedicine* **2016**, *11*, 3571–3583.

(30) Barriga, H. M. G.; Holme, M. N.; Stevens, M. M. Cubosomes; the next Generation of Smart Lipid Nanoparticles? *Angew. Chemie Int. Ed.* **2018**.

https://doi.org/10.1002/anie.201804067.

(31) Conn, C. E.; Mulet, X.; Moghaddam, M. J.; Darmanin, C.; Waddington, L. J.; Sagnella, S. M.; Kirby, N.; Varghese, J. N.; Drummond, C. Enhanced Uptake of an Integral Membrane Protein, the Dopamine D2L Receptor, by Cubic Nanostructured Lipid Nanoparticles Doped with Ni(II) Chelated EDTA Amphiphiles. *Soft Matter* **2011**, *7*, 567–578.

(32) Zabara, A.; Negrini, R.; Onaca-Fischer, O.; Mezzenga, R. Perforated Bicontinuous Cubic Phases with PH-Responsive Topological Channel Interconnectivity. *Small* **2013**, *9* (21), 3602–3609. https://doi.org/10.1002/smll.201300348.

(33) Rodrigues, L.; Kyriakos, K.; Schneider, F.; Dietz, H.; Winter, G.; Papadakis, C. M.; Hubert, M. Characterization of Lipid-Based Hexosomes as Versatile Vaccine Carriers. *Mol. Pharm.* **2016**, *13* (11), 3945–3954.

(34) Zhai, J.; Waddington, L. J.; Wooster, T. J.; Aguilar, M.-I.; Boyd, B. J. Revisiting β-Casein as a Stabilizer for Lipid Liquid Crystalline Nanostructured Particles. *Langmuir* **2011**, *27* (24), 14757–14766.

(35) Che, X.; Wang, Z.; Liu, Y.; Sun, Y.; Liu, H. Sustained Release of Nerve Growth Factor from Highly Homogenous Cubosomes Stabilized by B-Casein with Enhanced Bioactivity and Bioavailability. *RSC Adv.* **2016**, *6*, 114676–114684.

(36) Biffi, S.; Andolfi, C.; Caltagirone, C.; Garrovo, C.; Falchi, A. M.; Lippolis, V.; Lorenzon, A.; Macor, P.; Meli, V.; Monduzzi, M. Cubosomes for in Vivo Fluorescence Lifetime Imaging. *Nanotechnology* **2017**, *28*, 055102.

(37) Kim, H.; Sung, J.; Chang, Y.; Alfeche, A.; Leal, C. Microfluidics Synthesis of Gene

Silencing Cubosomes. *ACS Nano* **2018**, *12* (9), 9196–9205. https://doi.org/10.1021/acsnano.8b03770.

(38) Yanez Arteta, M.; Kjellman, T.; Bartesaghi, S.; Wallin, S.; Wu, X.; Kvist, A. J.; Dabkowska, A.; Székely, N.; Radulescu, A.; Bergenholtz, J.; et al. Successful Reprogramming of Cellular Protein Production through MRNA Delivered by Functionalized Lipid Nanoparticles. *Proc. Natl. Acad. Sci. U. S. A.* **2018**, *115* (15), E3351–E3360. https://doi.org/10.1073/pnas.1720542115.

(39) Cherezov, V.; Clogston, J.; Papiz, M. Z.; Caffrey, M. Room to Move: Crystallizing Membrane Proteins in Swollen Lipidic Mesophases. *J. Mol. Biol.* **2006**, *357* (5), 1605–1618.

(40) Cherezov, V. Lipidic Cubic Phase Technologies for Membrane Protein Structural Studies. *Curr. Opin. Struct. Biol.* **2011**, *21* (4), 559–566.

(41) Leung, S. S. W.; Leal, C. The Stabilization of Primitive Bicontinuous Cubic Phases with Tunable Swelling over a Wide Composition Range. *Soft Matter* **2019**, *15* (6), 1269–1277. https://doi.org/10.1039/C8SM02059K.

(42) Zabara, A.; Chong, J. T. Y.; Martiel, I.; Stark, L.; Cromer, B. A.; Speziale, C.; Drummond, C. J.; Mezzenga, R. Design of Ultra-Swollen Lipidic Mesophases for the Crystallization of Membrane Proteins with Large Extracellular Domains. *Nat. Commun. 2018 91* **2018**, *9* (1), 544. https://doi.org/10.1038/s41467-018-02996-5.

(43) Angelov, B.; Angelova, A.; Drechsler, M.; Garamus, V. M.; Mutafchieva, R.; Lesieur, S. Identification of Large Channels in Cationic PEGylated Cubosome Nanoparticles by

Synchrotron Radiation SAXS and Cryo-TEM Imaging. *Soft Matter* **2015**, *11*, 3686–3692.

(44) Leal, C.; Bouxsein, N. F.; Ewert, K. K.; Safinya, C. R. Highly Efficient Gene Silencing Activity of SiRNA Embedded in a Nanostructured Gyroid Cubic Lipid Matrix. *J. Am. Chem. Soc.* **2010**, *132* (47), 16841–16847. https://doi.org/10.1021/ja1059763.

(45) Kim, H.; Leal, C. Cuboplexes: Topologically Active SiRNA Delivery. *ACS Nano* **2015**, *9* (10), 10214–10226.

(46) Seddon, J. M.; Squires, A. M.; Conn, C. E.; Ces, O.; Heron, A. J.; Mulet, X.; Shearman, G. C.; Templer, R. H. Pressure-Jump X-Ray Studies of Liquid Crystal Transitions in Lipids. *Philos. Trans. R. Soc. A Math. Phys. Eng. Sci.* **2006**, *364* (1847), 2635–2655. https://doi.org/10.1098/rsta.2006.1844.

(47) Bruinsma, R. Elasticity and Excitations of Minimal Crystals. *J. Phys. II* **1992**, No. 2, 425–451.

(48) Cherezov, V.; Clogston, J.; Misquitta, Y.; Abdel-Gawad, W.; Caffrey, M. Membrane Protein Crystallization In Meso: Lipid Type-Tailoring of the Cubic Phase. *Biophys. J.* **2002**, *83* (6), 3393–3407.

(49) Anderson, D. M.; Gruner, S. M.; Leibler, S. Geometrical Aspects of the Frustration in the Cubic Phases of Lyotropic Liquid Crystals. *Proc. Natl. Acad. Sci.* **1988**, *85*, 5364–5368.

(50) Briggs, J.; Chung, H.; Caffrey, M. The Temperature-Composition Phase Diagram and Mesophase Structure Characterization of the Monoolein/Water System. *J. Phys. II* **1996**, *6* (5), 723–751.

(51) Pisani, M.; Bernstorff, S.; Ferrero, C.; Mariani, P. Pressure Induced Cubic-to-Cubic Phase Transition in Monoolein Hydrated System. *J. Phys. Chem. B* **2001**, *105*, 3109–3119.

(52) Shetty, K. N.; Latha, V. L.; Rao, R. N.; Nadimpalli, S. K.; Suguna, K. Affinity of a Galactose-Specific Legume Lectin from Dolichos Lablab to Adenine Revealed by X-Ray Cystallography. *Int. Union Biochem. Mol. Biol.* **2013**, *65* (7), 633–644.

TOC Graphic

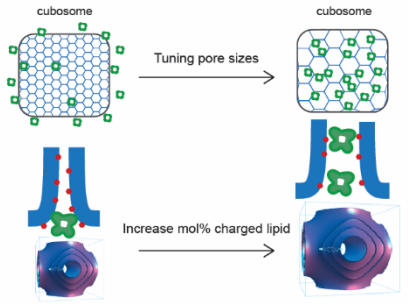
cubosome
cubosome
Tuning pore sizes
Increase mol% charged lipid